2015 IEEE 26th International Symposium on Personal, Indoor and Mobile Radio Communications - (PIMRC): Workshop on Wireless Communications in Millimeter Wave Bands

AoD and AoA Tracking with Directional Sounding Beam Design for Millimeter Wave MIMO Systems

Qiyou Duan†, Taejoon Kim†, Huang Huang‡, Kunpeng Liu‡, and Guangjian Wang‡
†Department of Electronic Engineering and State Key Laboratory of Millimeter Waves, City University of Hong Kong, Hong Kong
Email: qyduan.ee@my.cityu.edu.hk, taejokim@cityu.edu.hk
‡Huawei Technologies, Co. Ltd., Chengdu, P.R.C.
Email: huanghuang@huawei.com, liukunpeng@huawei.com, wangguangjian@huawei.com

***Abstract*—Millimeter wave multiple-input multiple-output (MIMO) systems equipped with large-sized array antennas have a great potential to boost the achievable data rates by leveraging large bandwidth available at the spectrum. In this paper, we focus on the angle of departure (AoD) and angle of arrival (AoA) tracking problem for temporally correlated sparse millimeter wave MIMO channels. With the beam space MIMO channel modeling, a low complexity two-sided channel sounding scheme for the AoD and AoA tracking is investigated. The adoption of the sparse beam space MIMO channel representation eventually converts the AoD and AoA estimation problem to the support recovery problem. For the support recovery, we employ an iterative soft thresholding algorithm which is broadly referred to as the approximate message passing (AMP) algorithm. The support recovery performance of the AMP, however, suffers from serious deterioration especially at the low SNR regime. To remedy, several directional sounding beam design schemes are proposed to ameliorate the performance of the channel tracking at the low SNR. Simulation results demonstrate that the proposed AoD and AoA tracking outperforms other benchmark schemes when compared in a low SNR setting.**

I. Introduction

The ever-increasing data rate demand brings various challenges to traditional microwave multiple-input multiple-output (MIMO) systems. Recently, the millimeter wave spectrum has attracted tremendous interest from both the industry and academia because of the large bandwidth underutilized in the spectrum. In the millimeter wave, the large number of array antennas can be packed in a small form factor making large-scale multiple-input multiple-output (MIMO) feasible [1], [2]. Initial work in the millimeter wave MIMO focuses on large dimensional analog beamforming [3]–[5] and demonstrates that significant throughput gain is possible by employing adaptive beams at the transmitter and receiver to overcome the severe path loss. The hybrid analog-digital MIMO precoding and combing techniques have also been proposed in [6], [7], which further enhance the spectral efficiency by customizing both the analog and digital precoder/combiner.

In the millimeter wave MIMO, it is essential to get accurate channel estimates at both the transmitter and the receiver to facilitate advanced precoding and combining techniques. Traditionally, a block of channel uses are spent to sound the channel and extract useful channel state information (CSI) during a fixed coherent channel block. Since only limited paths are presented in the sparse millimeter wave MIMO channels, channel estimation problem can be converted into an effective channel path searching problem. This motivates the adoption of the beam space MIMO channel representation [8] to model the sparse millimeter wave MIMO channel. The beam space MIMO representation has been exploited to analyze the achievable throughput of the millimeter wave MIMO channels [9]. Recently, a low complexity virtual angle of departure (AoD) and angle of arrival (AoA) estimation technique leveraging the beam space MIMO channel representation has been proposed [10].

Temporal correlation always exists between channel realizations in practical MIMO channels. Unlike the independent fading channel, the current CSI is dependent on the past CSI in a temporally correlated channel. Hence, provided substantial temporal correlation, past CSI can be reused to further refine the quality of the current channel estimate. This procedure is often referred to as channel tracking. In a rich scattering MIMO channel, the channel tracking problem has been investigated, for instance, by employing differential feedback [11], stochastic perturbation [12], and geodesic fitting [13] techniques. With the substantial sparsity presented in the millimeter wave MIMO channel, the extension of aforementioned techniques [11]–[13], that is customized to small dimensional rich scattering MIMO channel, to the millimeter wave channel is not feasible. Thus far, no work investigating the large dimensional, but substantially sparse millimeter wave channel tracking technique leveraging sparse channel representation like the beam space MIMO [8], has been reported.

In this paper, based on the beam space MIMO channel model, we present a low complexity two-sided AoD and AoA tracking framework. Adoption of the sparse channel representation [8] effectively formulate the AoD and AoA estimation problem as the support recovery problem. An uncomplicated iterative approximate message passing (AMP) algorithm is employed and modified in our work to track the temporal evolution of AoD and AoA. A preferred sounding beam property that guarantees high support recovery rate is defined by the isometry property [14], [15]. This property motivates the use of omni-directional sounding beams. However, the omni-directional beam suffers from performance deterioration at the low SNR. Several directional sounding beam design

The authors at the City University of Hong Kong were supported in part by Huawei Technologies.

978-1-4673-6782-0/15/$31.00 ©2015 IEEE

techniques, which adopt the direction of the sounding beam to the temporal AoD and AoA evolution statistics, are proposed. When compared to other benchmarking schemes, the proposed approaches exhibit enhanced achievable throughput gain.

II. System Model and Beam Space MIMO Channel Representation

In this section, we present the signal model of the millimeter wave MIMO hybrid analog-digital precoding and combining system and introduce the temporally correlated channels based on the beam space MIMO channel representation.

A. Signal Model

Consider a point-to-point MIMO channel with the channel coherence block length T_B (channel uses). We assume time division duplexing (TDD) in which the transmitter and receiver can exploit channel reciprocity. The transmitter is equipped with N_T antennas and N_{BS} RF chains, while the receiver is equipped with N_R antennas and N_{MS} RF chains. Let N_D denotes the number of data streams and $N_D \leq \min(N_{BS}, N_{MS}) \ll \min(N_T, N_R)$. The channel output $\mathbf{y}^\tau \in \mathbb{C}^{N_D \times 1}$ at the channel block τ in the downlink is modeled via (the channel block index τ is omitted for conciseness)

$$\mathbf{y} = \mathbf{W}_{BB}^* \mathbf{W}_{RF}^* \mathbf{H} \mathbf{F}_{RF} \mathbf{F}_{BB} \mathbf{s} + \mathbf{W}_{BB}^* \mathbf{W}_{RF}^* \mathbf{n}, \quad (1)$$

where $\mathbf{W}_{RF} \in \mathbb{C}^{N_R \times N_{MS}}$ and $\mathbf{W}_{BB} \in \mathbb{C}^{N_{MS} \times N_D}$ represent the analog combiner and digital combiner, respectively, at the receiver. The $\mathbf{H} \in \mathbb{C}^{N_R \times N_T}$ is the millimeter wave MIMO channel from the transmitter to receiver. The $\mathbf{F}_{RF} \in \mathbb{C}^{N_T \times N_{BS}}$ and $\mathbf{F}_{BB} \in \mathbb{C}^{N_{BS} \times N_D}$ are, respectively, the analog precoder and digital precoder at the transmitter. The ith row and jth column elements of $\mathbf{F}_{RF}$ and $\mathbf{W}_{RF}$, i.e., $F_{RF}^{(i,j)}$ and $W_{RF}^{(i,j)}$, are constrained to

$$\left|F_{RF}^{(i,j)}\right| = \frac{1}{\sqrt{N_T}}, \text{and } \left|W_{RF}^{(i,j)}\right| = \frac{1}{\sqrt{N_R}}, \forall i, j, \quad (2)$$

representing the phase shifters of analog precoder and combiner, whose phase shifting values are quantized and chosen in a finite set. The $\mathbf{s} \in \mathbb{C}^{N_D \times 1}$ in (1) is the transmitted signal subject to the power constraint $\|\mathbf{F}_{RF}\mathbf{F}_{BB}\mathbf{s}\|_2^2 = 1$. The $\mathbf{n} \in \mathbb{C}^{N_R \times 1}$ is the additive noise with each entry independently and identically distributed (i.i.d.) as $\mathcal{CN}(0, \sigma^2)$.

B. Beam Space MIMO Channel Representation

A physical channel representation has been conventionally used in the previous work, e.g., [4], [6], [7]. Recent studies have demonstrated that practical millimeter wave MIMO channel exhibits substantial sparsity [1], [2]. The substantial sparsity and the limited resolution of the beam pattern generated by the quantized phased shifting values advocate the use of the beam space MIMO channel representation in [8], in which the channel $\mathbf{H}$ is represented by

$$\mathbf{H} = \mathbf{D}_r \mathbf{H}_v \mathbf{D}_t^*, \quad (3)$$

where $\mathbf{D}_r \in \mathbb{C}^{N_R \times N_R}$ and $\mathbf{D}_t \in \mathbb{C}^{N_T \times N_T}$ are unitary discrete Fourier transform (DFT) matrices, while $\mathbf{H}_v \in \mathbb{C}^{N_R \times N_T}$ is the virtual channel matrix of $\mathbf{H}$. This representation in (3) is obtained by uniformly quantizing the physical angles of departure and arrival [8].

Since the matrices $\mathbf{D}_t$ and $\mathbf{D}_r$ are unitary, one can write $\mathbf{H}_v = \mathbf{D}_r^* \mathbf{H} \mathbf{D}_t$, meaning that $\mathbf{H}_v$ captures the sparse CSI of $\mathbf{H}$. Distinct coefficients of $\mathbf{H}_v$ are assumed to be i.i.d. [8]. Provided the sparse representation, we would rather track the AoDs and AoAs of $\mathbf{H}_v$ than track the effective channel paths in $\mathbf{H}$.

C. Temporal Beam Space Evolution

To model the AoD and AoA evolution from current channel block to next channel block, we employ x to indicate the number of supports in $\mathbf{H}_v$ and define an element in the support of $\mathbf{H}_v$ (i.e., the nonzero elements of $\mathbf{H}_v$) as the binary indicator $s_{H_{v,k}} \in \{0, 1\}, k = 1, \ldots, x$. More specifically, $s_{H_{v,k}}=1$ if $|H_{v,k}|>0$ and $s_{H_{v,k}}=0$, otherwise. This treatment shows that tracking the AoDs and AoAs of the sparse $\mathbf{H}_v$ is equivalent to tracking the support of $\mathbf{H}_v$.

In practice, there always exists temporal correlation between channel realizations. We exploit this fact and model the temporal evolution of $\mathbf{H}_v$. The temporal evolution in our system model consists of two parts. The first part is the support evolution that models the slow variation of supports $s_{H_{v,k}}|_{k=1}^{x}$ in $\mathbf{H}_v$ from channel block τ to $\tau + 1$. The support transition probability is defined as

$$p = \Pr\{\Omega(H_{v,k}^{\tau+1}) \in \mathcal{P}_k^{\tau+1} \mid \Omega(H_{v,k}^{\tau}) \in \mathcal{P}_k^{\tau}\}, \ k = 1, \ldots, x, \quad (4)$$

where $\Omega(\cdot)$ represents the operator which extracts the row and column index (i.e., position) of the support coefficient. The set $\mathcal{P}_k^\tau = \{(i, j)\}$ denotes the original position (ith row and jth column in $\mathbf{H}_v$) of the kth support at τth channel block, while $\mathcal{P}_k^{\tau+1} = \{(i-1, j-1), (i-1, j), (i-1, j+1), (i, j-1), (i, j+1), (i+1, j-1), (i+1, j), (i+1, j+1)\}$ is the set containing all possible support evolution positions at $\tau + 1$. Conversely, $1-p$ denotes the probability of support staying in the original position. The second part is the channel coefficient evolution in which the evolution of the propagation path gains is modeled via the first order Gauss-Markov process as

$$H_{v,k}^{\tau+1} = \rho H_{v,k}^{\tau} + \sqrt{1-\rho^2} v^{\tau+1}, \quad (5)$$

where the ρ $(0 \leq \rho \leq 1)$ is the temporal correlation coefficient. The $v^{\tau+1}$ is the innovation process drawn from $\mathcal{CN}(0, 1)$ and independent from $H_{v,k}^{\tau}$.

III. AoD and AoA Tracking

The performance of the AoD and AoA estimation can be enhanced by refining the current estimate using the past CSI, motivating the need for an efficient AoD and AoA tracking technique. In this section, we investigate, based on the beam space MIMO channel model described in the previous section, a low-complexity AoD and AoA tracking technique.

A. Two-sided Sounding Scheme for AoD and AoA Estimation

Directly dealing with the $\mathbf{H}_v \in \mathbb{C}^{N_R \times N_T}$ could cause prohibitively complex matrix operations for a large dimension (e.g., $N_T N_R \approx 10^6$). Hence, we consider a low overhead framework and adopt the two-sided sounding technique in [10].

To simplify the description, we focus, in this subsection, on one channel block and omit the channel block index τ. The two-sided framework exploits the channel reciprocity. In particular, channel sounding is divided into two parts: 1) N_R-dimensional AoA estimation at the receiver via downlink sounding; and 2) N_T-dimensional AoD estimation at the transmitter via uplink sounding.

The downlink sounding for AoA estimation is equivalent to the row support recovery of $\mathbf{H}_v$. The receiver samples the row subspace during the first $K/2$ (where K denotes the number of channel uses allocated to channel sounding) channel uses as

$$\mathcal{S}_{row} = \left\{ i \mid \left| \sum_{j=1}^{N_T} H_v^{(i,j)} \right| > 0,\ i = 1, \ldots, N_R \right\}. \tag{6}$$

The uplink sounding for AoD estimation is the column support recovery of $\mathbf{H}_v$ at the transmitter through the remaining $K/2$ channel uses yielding the column support

$$\mathcal{S}_{column} = \left\{ j \mid \left| \sum_{i=1}^{N_R} H_v^{(i,j)} \right| > 0, j = 1, \ldots, N_T \right\}. \tag{7}$$

In what follows, we describe the downlink sounding only since the uplink sounding procedures are exactly same as that of the downlink sounding because of the channel reciprocity.

In the downlink sounding, the transmitter fixes the beam using a beamformer $\mathbf{f}_t$. The receiver samples the row subspace of $\mathbf{H}_v$ using the analog combiner $\mathbf{W}_r = [\mathbf{W}_1 \cdots \mathbf{W}_{K/2}] \in \mathbb{C}^{N_R \times M}$, in which $\mathbf{W}_o \in \mathbb{C}^{N_R \times N_{MS}}, o = 1, \ldots, K/2$, and $M = N_{MS} K/2 \ll N_R$ is the number of samples. Collecting the received samples in a vector $\mathbf{y}_d = [\mathbf{y}_1^T \cdots \mathbf{y}_{K/2}^T]^T \in \mathbb{C}^{M \times 1}$ yields

$$\mathbf{y}_d = \mathbf{W}_r^* \mathbf{D}_r \mathbf{H}_v \mathbf{D}_t^* \mathbf{f}_t + \mathbf{n}_d, \tag{8}$$

where $\mathbf{n}_d = [(\mathbf{W}_1^* \mathbf{n}_1)^T \cdots (\mathbf{W}_{K/2}^* \mathbf{n}_{K/2})^T]^T \in \mathbb{C}^{M \times 1}$. Define $\mathbf{A} \triangleq \mathbf{W}_r^* \mathbf{D}_r \in \mathbb{C}^{M \times N_R}$ as the sensing matrix, and $\mathbf{h}_d \triangleq \mathbf{H}_v \mathbf{D}_t^* \mathbf{f}_t \in \mathbb{C}^{N_R \times 1}$ as the row support vector, which succinctly leads to

$$\mathbf{y}_d = \mathbf{A}\mathbf{h}_d + \mathbf{n}_d. \tag{9}$$

The expression in (9) elucidates that the AoA estimation problem is indeed equivalent to the support recovery problem of $\mathbf{h}_d$ [10].

B. Omni-directional Sounding Beam Design

Given the signal model in (9), an appropriate sensing matrix $\mathbf{A}$ is of great importance towards the success of support recovery. In the compressed sensing literature, a property of a good sensing matrix is referred to as the isometry property [14], [15], in which $\mathbf{A}^*\mathbf{A}$ is required to be close to the identity matrix. The intuition behind the isometry property is to uniformly sample the source vector to guarantee uniformly high recovery rate. This observation can be extended to our AoD and AoA estimation problem and motivates us to use omni-directional beams to uniformly sample the angular beam space. In order to find the appropriate sensing matrix $\mathbf{A}$ that satisfies the analog constraint in (2) with the quantized phase values, we propose to adopt a polyphase (i.e., chirp-type) constant envelope sequence, the Zadoff-Chu (ZC) sequence [16]. Since the ZC sequence is a chirp-type, it produces a uniform and omni-directional power profile in angular domain.

The sounding beam $\mathbf{f}_t$ design at the transmitter is firstly discussed. The $\mathbf{f}_t$ is designed using ZC sequence as

$$f_{t,j} = e^{j\pi q(j-1)j/N_T} / \sqrt{N_T},\ j = 1, \ldots, N_T, \tag{10}$$

where $q \in \{1, \ldots, N_T - 1\}$ denotes the root of the sequence and the length of sequence N_T is prime. Since the DFT of ZC sequence is also a ZC sequence [17], the $\mathbf{D}_t \mathbf{f}_t$ can also uniformly sample $\mathbf{H}_v$. Following the same reasoning, the combiner $\mathbf{W}_r$ in (8) is constructed using ZC sequences. Suppose that the first column of $\mathbf{W}_r$, i.e., $\mathbf{w}_1$, has entries as $w_{1,i} = e^{j\pi q(i-1)i/N_R} / \sqrt{N_R}, i = 1, \ldots, N_R$. Then, the kth column of $\mathbf{W}_r$ is designed as the cyclical shift of $\mathbf{w}_1$ by $k-1$ samples, i.e.,

$$w_{k,i} = e^{j\pi q(i-(k-1)-1)(i-(k-1))/N_R} / \sqrt{N_R},\ i = 1, \ldots, N_R$$

for $k = 1, \ldots, M$.

C. AMP with Soft Thresholding

Provided the omni-directional sounding beams in Section III.B, we adopt a low-complexity support recovery algorithm, the so called approximate massage passing with soft thresholding (AMP-ST) [18]. The original AMP-ST in [18] considers column normalization of the sensing matrix $\mathbf{A}$. However, as seen from Section III.B, our design of $\mathbf{A}$ considers row normalization. Hence, we modify the sensing matrix such that $\mathbf{A}_d = \sqrt{N_R/M}\mathbf{A} = \sqrt{N_R/M}\mathbf{W}_r^*\mathbf{D}_r$ so that $\sum_{r=1}^{M} |A_d^{(r,c)}|^2 = 1, \forall c$. Since the normalization should be applied at the MS, it is, in practice, done by $\tilde{\mathbf{y}}_d = \sqrt{N_R/M}\mathbf{y}_d$.

The AMP algorithm adapted to our signal model is described as follows. Starting with initial conditions for the first channel block, i.e., $\tau = 1$: $\mathbf{h}_d^{0,\tau} = \mathbf{0}$, $\mathbf{z}^{0,\tau} = \tilde{\mathbf{y}}_d^{\tau}$, and $\epsilon^{0,\tau} \gg \frac{1}{M} \|\tilde{\mathbf{y}}_d^{\tau}\|_2^2$. The algorithm iterates for $i = 0, \ldots, I-1$ (where I indicates the number of the iterations) as

$$\boldsymbol{\mu}^{i,\tau} = \mathbf{A}_d^* \mathbf{z}^{i,\tau} + \mathbf{h}_d^{i,\tau} \tag{11}$$

$$\mathbf{h}_d^{i+1,\tau} = \eta(\boldsymbol{\mu}^{i,\tau}; \epsilon^{i,\tau}) \tag{12}$$

$$\mathbf{z}^{i+1,\tau} = \tilde{\mathbf{y}}_d^{\tau} - \mathbf{A}_d \mathbf{h}_d^{i+1,\tau} + \frac{1}{M} \sum_{l=1}^{N_r} \frac{\partial \eta(\mu_l^{i,\tau}, \epsilon^{i,\tau})}{\partial \mu_l^{i,\tau}} \mathbf{z}^{i,\tau} \tag{13}$$

$$\epsilon^{i+1,\tau} = \sqrt{\frac{\|\mathbf{A}_d^* \mathbf{z}^{i+1,\tau}\|_2^2}{M}} \tag{14}$$

In (13), the vector $\mathbf{z}^{i+1,\tau}$ represents the approximate estimate error in the compressed M-dimensional space at the $i+1$th iteration [18]. We set the threshold value as standard deviation of the projected estimation error $\mathbf{z}^{i+1,\tau}$ onto the N_R-dimensional source subspace. The function $\eta(\mu_l; \epsilon)$ with the

soft thresold value ϵ is defined as [19]

$$\eta(\mu_l;\epsilon)=\begin{cases}\mu_l-\epsilon\frac{\mu_l}{|\mu_l|}, & \text{if } |\mu_l|>\epsilon;\\ 0, & \text{if } |\mu_l|\le\epsilon,\end{cases} \tag{15}$$

where μ_l denotes the lth entry of $\boldsymbol{\mu}$. After the Ith iteration, the algorithm returns the estimate $\hat{\mathbf{h}}_d^{I,\tau}$.

D. Block Iteration for Channel Tracking

The AoD and AoA tracking algorithm at $\tau+1$th channel block can leverage the past CSI $\hat{\mathbf{h}}_d^{I,\tau}$. The updated initial conditions at $\tau+1$th channel block can be set to

$$\mathbf{h}_d^{0,\tau+1}=\hat{\mathbf{h}}_d^{I,\tau} \tag{16}$$

$$\mathbf{z}^{0,\tau+1}=\mathbf{y}_d^{\tau+1}-\mathbf{A}_d\mathbf{h}_d^{0,\tau+1} \tag{17}$$

$$\epsilon^{0,\tau+1}\gg\sqrt{\frac{\|\mathbf{A}_d^*\mathbf{z}^{0,\tau+1}\|_2^2}{M}}. \tag{18}$$

Given the updated initial conditions in (16)-(18), the modified AMP-ST approach described in (11)-(14) is applied to recover the row support in $\mathbf{H}_v^{\tau+1}$.

IV. Directional Sounding Beam Design

The tracking technique employing the omni-directional sounding beam presented in the previous section could show a reliable estimation performance at high SNR, because the isometry property of the sensing matrix [14], [15] is derived assuming a high SNR setting. As will be seen in Section V, the performance of the AMP based on the omni-direcitonal beams is deteriorated in low SNR. It is practically important to device techniques that enhance the low SNR performance since energy saving is a critical issue of the complicated millimeter wave MIMO circuitry.

To enhance the low SNR performance, we propose to use directional sounding beams combined with the AMP tracking algorithm described in Section III.C. We describe multiple directional sounding beam design techniques taking the downlink sounding as an example. The exactly same procedures apply to the uplink sounding. We divide our discussion into the directional transmit sounding beam design and the directional receive sounding beam design. We first describe the former.

A. Directional Transmit Sounding Beam Design

There are three schemes proposed for the directional transmit sounding beam design.

1) Scheme 1: The first scheme designs the directional transmit beam in (8) in a form

$$\mathbf{f}_t=\frac{\mathbf{D}_t\mathbf{S}\mathbf{s}_t}{\|\mathbf{D}_t\mathbf{S}\mathbf{s}_t\|_2}=\frac{\mathbf{D}_t\hat{\mathbf{s}}_t}{\|\mathbf{D}_t\hat{\mathbf{s}}_t\|_2}, \tag{19}$$

where $\mathbf{S}\in\mathbb{C}^{N_T\times N_{BS}}$ denotes the selection matrix and the vector $\mathbf{s}_t\in\mathbb{C}^{N_{BS}\times 1}$ contains AoD supports estimated in the previous channel block, and $\hat{\mathbf{s}}_t\in\mathbb{C}^{N_T\times 1}$ is the extended support vector, i.e., $\hat{\mathbf{s}}_t=\mathbf{S}\mathbf{s}_t$. Details about designing each part are provided in the following four steps:

- After the AoD support recovery, which returns the estimate $\hat{\mathbf{h}}_u^{I,\tau}$ for the uplink sounding, keep the estimated channel $\hat{\mathbf{h}}_u=\hat{\mathbf{h}}_u^{I,\tau}$ sorted in descending order as
$$|\hat{h}_{u,j_1}|\ge|\hat{h}_{u,j_2}|\ge\cdots\ge|\hat{h}_{u,j_{\hat{x}}}|\ge\cdots\ge|\hat{h}_{u,j_{N_T}}|,$$
where j_i denotes the index of the ith dominant entry, and $\hat{x}$ is the cardinality of nonzero elements in the estimated channel vector $\hat{\mathbf{h}}_u$.
- If $\hat{x}\le N_{BS}$ and the support set is $\mathcal{Q}=\{j_1,j_2,\ldots,j_{\hat{x}}\}$, the $\hat{x}$ nonzero elements is mapped to $\mathbf{s}_t\in\mathbb{R}^{N_{BS}\times 1}$ with making up $N_{BS}-\hat{x}$ zero entries. Specifically speaking, the first $\hat{x}$ entries of $\mathbf{s}_t$ are set to 1 and the remaining entries are set to zeros. When $\hat{x}>N_{BS}$, the support set is $\mathcal{Q}=\{j_1,j_2,\ldots,j_{N_{BS}},\ldots,j_{\hat{x}}\}$. The $\mathbf{s}_t$ is constructed, in this case, by setting all entries to ones.
- Given the $\mathbf{s}_t$, we design the selection matrix $\mathbf{S}$ by adapting to the support evolution statistics in Section II.C. The ith column of $\mathbf{S}$ is designed as $[\mathbf{S}]_{:,i}=[0\ 0\ \ldots\ 0\ \varepsilon\ 1\ \varepsilon\ 0\ \ldots\ 0]^T\in\mathbb{C}^{N_T\times 1}$, where the 1 entry denotes the j_ith element in $\mathcal{Q}$ and $\varepsilon\le 1$ represents the scaling parameter for support extension, which is a function of the support transition probability (4).
- Combining $\mathbf{s}_t$ and $\mathbf{S}$ yields the extended support vector $\hat{\mathbf{s}}_t$. The directional transmit sounding beam adapted to support evolution is then given by $\mathbf{f}_t=\mathbf{D}_t\mathbf{S}\frac{\mathbf{s}_t}{\|\mathbf{D}_t\mathbf{S}\mathbf{s}_t\|_2}$.

As seen from (19), Scheme 1 forms a directional beam as a linear combination of the partial DFT matrix. Each column of DFT matrix produces a narrow beam. Depending on the regulatory constraints on the bands employed, the allowed beam width is in general strictly constrained. To address, we introduce Scheme 2 that generates a directional beam as a linear combination of omni-directional beams.

2) Scheme 2: The ZC sequences are adopted as omni-directional beams to produce a directional beam. The directional beam is constructed by solving the optimization problem

$$\mathbf{f}_t=\underset{\mathbf{f}_t=\mathbf{Z}_t^{opt}\mathbf{x}_t,\mathbf{x}_t\in\mathbb{C}^{N_{BS}\times 1}}{\operatorname{argmin}}\|\mathbf{Z}_t^{opt}\mathbf{x}_t-\mathbf{D}_t\hat{\mathbf{s}}_t\|_2, \tag{20}$$

where $\mathbf{Z}_t^{opt}=[\mathbf{Z}_t]_{:,i_{1:N_{BS}}}\in\mathbb{C}^{N_T\times N_{BS}}$ consists of N_{BS} columns chosen from ZC-sequence matrix $\mathbf{Z}_t\in\mathbb{C}^{N_T\times N_T}$ according to the following order:

$$|\boldsymbol{\theta}_{i_1}|\ge\cdots\ge|\boldsymbol{\theta}_{i_{N_{BS}}}|\ge\cdots\ge|\boldsymbol{\theta}_{i_{N_T}}|.$$

where $\boldsymbol{\theta}=\mathbf{Z}_t^*\mathbf{D}_t\hat{\mathbf{s}}_t\in\mathbb{C}^{N_T\times 1}$. The ZC sequence matrix $\mathbf{Z}_t$ has kth column formed by cyclic-shifting a ZC sequence of length N_T by $k-1$ samples. This construction ensures that $\mathbf{Z}_t^*\mathbf{Z}_t=\mathbf{Z}_t\mathbf{Z}_t^*=\mathbf{I}$. Then the solution of the problem in (20) is attained as

$$\mathbf{f}_t^\star=\mathbf{Z}_t^{opt}\mathbf{x}_t^\star=\mathbf{Z}_t^{opt}(\mathbf{Z}_t^{opt*}\mathbf{Z}_t^{opt})^{-1}\mathbf{Z}_t^{opt*}\mathbf{D}_t\hat{\mathbf{s}}_t. \tag{21}$$

3) Scheme 3: In Scheme 1 and Scheme 2, the resolution of the directional beam is restricted by the limited number of RF chains. In order to get rid of the limitation but also provide effective directional sounding beams, Scheme 3 is proposed. The key idea of this scheme is to superpose directional beams

and project the superposed beam onto the complex circle manifold. The detailed procedures are described as follows.

- Extend the support without any constraint on the number of RF chains. Suppose the support set is $\mathcal{Q} = \{j_1, \ldots, j_i, \ldots, j_{\hat{x}}\}$.
- Superpose all the beams (selected from DFT matrix) with respect to the extended support as

$$\mathbf{f}_0 = \sum_{i=1}^{\hat{x}} [\mathbf{D}_t]_{:,j_i} + \varepsilon \sum_{i=1}^{\hat{x}} [\mathbf{D}_t]_{:,j_i-1} + \varepsilon \sum_{i=1}^{\hat{x}} [\mathbf{D}_t]_{:,j_i+1} \in \mathbb{C}^{N_T \times 1}$$

  where $\varepsilon \leq 1$ is similarly defined as it in Scheme 1.
- Design the quantized directional beam. The idea is to project the superposed beam $\mathbf{f}_0$ onto the complex circle manifold (e.g., array manifold) and quantize the phase values. Denote the ith entry of $\mathbf{f}_0$ as $f_{0,i} = |f_{0,i}|e^{j\theta_{0,i}}$. The projection of $\mathbf{f}_0$ onto the complex circle manifold is done element-wise, yielding $f_{0,i} = 1/\sqrt{N_T}e^{j\theta_{0,i}}$. Given the quantization set $\mathcal{Q}_{N_T} = \{\theta_m \mid \theta_m = 2\pi(m-1)/N_T,\ m = 1, \ldots, N_T\}$ with the cardinality N_T, the quantizer finds $\theta_{q,i}$ such that

$$\theta_{q,i} = \underset{\theta \in \mathcal{Q}_{N_T}}{\operatorname{argmin}} |\theta - \theta_{0,i}|^2,$$

  leading to $f_{t,i} = 1/\sqrt{N_T}e^{j\theta_{q,i}}$.

B. Directional Receive Sounding Beam Design

Directional sounding beam design at the receiver is similar to the methodology described in Scheme 1 in Section IV.A. The procedures are summarized as follows.

- Given the estimated $\hat{\mathbf{h}}_d = \hat{\mathbf{h}}_d^{I,\tau}$, extract the support $\mathcal{Q} = \{j_1, j_2, \ldots, j_{\hat{x}}\}$.
- Construct the extended amplitude vector $\hat{\mathbf{h}}_d^{ext} \in \mathbb{C}^{N_R \times 1}$ based on the support evolution statistics in Section II.C using the scaling parameter $\varepsilon \leq 1$. For the original ith $(i = 1, \ldots, \hat{x})$ support, construct $\hat{\mathbf{h}}_d^{ext}$ such that $\hat{h}_{d,j_i}^{ext} = |\hat{h}_{d,j_i}|$ and $\hat{h}_{d,j_i-1}^{ext} = \hat{h}_{d,j_i+1}^{ext} = \varepsilon|\hat{h}_{d,j_i}|$. For $j \notin \mathcal{Q}$, $\hat{h}_{d,j_i}^{ext} = 0$.
- Keep the extended support sorted in descending order

$$\hat{h}_{d,j_1}^{ext} \geq \hat{h}_{d,j_2}^{ext} \geq \cdots \geq \hat{h}_{d,j_{\hat{x}}}^{ext} \geq \cdots \geq \hat{h}_{d,j_{\hat{x}^{ext}}}^{ext}.$$

- Design the directional beams at the receiver side according to two distinct cases: 1) $\hat{x}^{ext} \leq M$, the directional receive beam is constructed as

$$\mathbf{W}_r = [\mathbf{W}_1\ \mathbf{W}_2] \in \mathbb{C}^{N_R \times M}, \tag{22}$$

  where $\mathbf{W}_1 = [\mathbf{D}_r]_{:,j_{1:\hat{x}^{ext}}} \in \mathbb{C}^{N_R \times \hat{x}^{ext}}$, and $\mathbf{W}_2 = [\mathbf{Z}_r]_{:,I_r(1:M-\hat{x}^{ext})} \in \mathbb{C}^{N_R \times (M-\hat{x}^{ext})}$. The I_r is random permutation with dimension N_R, while the $\mathbf{D}_r$ and $\mathbf{Z}_r$ are the DFT matrix and ZC-sequence matrix, respectively. 2) $\hat{x}^{ext} > M$, then the design of directional receive beam is

$$\mathbf{W}_r = \mathbf{W} = [\mathbf{D}_r]_{:,j_{1:M}} \in \mathbb{C}^{N_R \times M}. \tag{23}$$

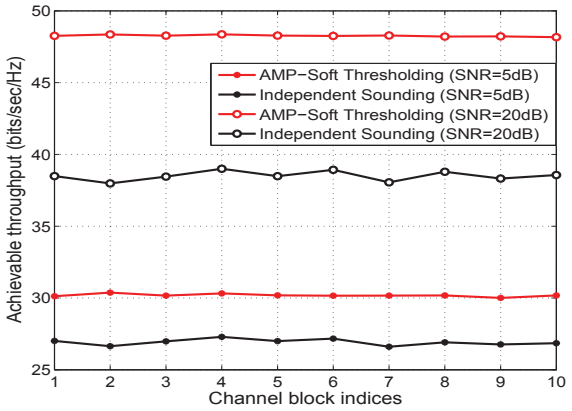

Fig. 1. Comparison of achievable throughputs of the AMP-ST with omni-directional beams and IS scheme for different SNRs.

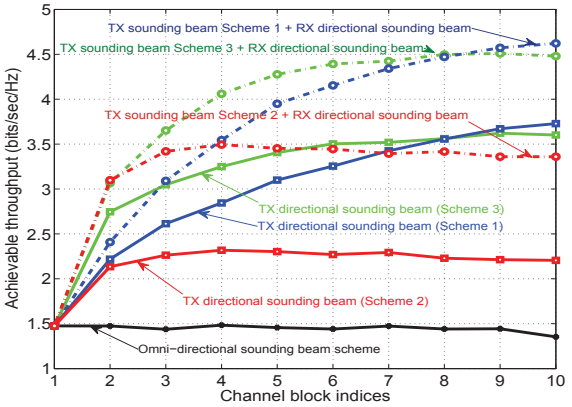

Fig. 2. Comparison of achievable throughput for the proposed directional sounding beam design schemes.

V. Simulation Results

In this section, numerical simulations are carried out to demonstrate the achievable throughput of the proposed techniques. The tracking capability is evaluated for 10 channel blocks. The average number of effective paths is set to 3 ensuring the sparse millimeter wave channel. The support transition probability p in (4) and temporal correlation coefficient parameter ρ in (5) are set to 0.05 and 0.95, respectively. We consider the carrier frequency of 72GHz and the mobile velocity of receiver $v = 5$km/h whose maximum Doppler frequency is 333Hz. Then, the length of channel block amounts to 0.3ms assuming that the channel block length is set to 10% (with sufficient coherency) of channel coherence time. We employ OFDM technique with 1024 FFT size and bandwidth of 1GHz. The OFDM symbol duration is calculated as $\frac{1024}{1GHz} \approx 1$us, implying that about $T_B = 300$ channel uses during one channel block can be utilized by the system.

Fig.1 compares the achievable throughputs of the proposed AMP-ST using omni-directional beams and the independent sounding (IS) technique for $N_R = N_T = 127$, $N_{BS} =$

$N_{MS} = 8$, and $M = 64$, and thus, $K = \lceil \frac{M}{N_{RF}} \rceil \times 2 = 16$. The IS scheme sounds randomly designed beam pairs at the transmitter and receiver, and choose the best beam pair. For the IS scheme, we set $K = 30$ for the fair comparison. In Fig.2, we compares the performance of proposed schemes with omni-directional sounding beam and directional sounding beam in a low SNR setting, in which we choose $N_R = N_T = 61$, $N_{BS} = 4$, $N_{MS} = 2$, $M = 40$, and thus $K = \lceil \frac{M}{N_{BS}} \rceil + \lceil \frac{M}{N_{MS}} \rceil = 30$, and SNR$= -10$dB.

As seen from Fig.1, the proposed AoD and AoA tracking algorithm with the omni-directional beam significantly outperforms the IS scheme in high SNR. The curves in Fig.2 indicate that the directional sounding beam design schemes all show better performance compared to the omni-directional beam scheme. Indeed, the performance enhancement of the directional beam design is substantial compared to the omni-directional beam design. It is also observed through extensive simulations that the performance trends of both the directional and omni-directional beam design are compatible each other at high SNR regime.

VI. Conclusions

The AoD and AoA tracking techniques leveraging the sparse channel representation, the beam space MIMO channel representation, were proposed by modifying the conventional AMP-ST algorithm with analog constrained omni-directional sounding beams and, as well, directional sounding beams. The directional sounding beam design is proposed to adapt the concentration of the beam power in angular domain to the AoD and AoA evolution statistics. Numerical evaluation illustrates that the presented AoD and AoA tracking scheme outperforms the independent sounding (IS) scheme significantly in high SNR regime. Moreover, the directional beam adaptation aiming at enhancing the performance at low SNR regime show substantially better channel tracking performance than the omni-directional beam design.

References

[1] J. Brady, N. Behdad, and A. Sayeed, "Beamspace MIMO for millimeter-wave communications: System architecture, modeling, analysis, and measurements," *IEEE Transactions on Antennas and Propagation*, vol. 61, no. 7, pp. 3814–3827, July 2013.

[2] T. Rappaport, S. Sun, R. Mayzus, H. Zhao, Y. Azar, K. Wang, G. Wong, J. Schulz, M. Samimi, and F. Gutierrez, "Millimeter wave mobile communications for 5G cellular: It will work!" *IEEE Access*, vol. 1, pp. 335–349, 2013.

[3] J. Wang, Z. Lan, C. Pyo, T. Baykas, C. Sum, M. Rahman, J. Gao, R. Funada, F. Kojima, H. Harada, and S. Kato, "Beam codebook based beamforming protocol for multi-Gbps millimeter-wave WPAN systems," *IEEE Journal on Selected Areas in Communications*, vol. 27, no. 8, pp. 1390–1399, Oct. 2009.

[4] S. Hur, T. Kim, D. Love, J. Krogmeier, T. Thomas, and A. Ghosh, "Millimeter wave beamforming for wireless backhaul and access in small cell networks," *IEEE Transactions on Communications*, vol. 61, no. 10, pp. 4391–4403, Oct. 2013.

[5] J. Song, S. Larew, D. Love, T. Thomas, and A. Ghosh, "Millimeter wave beam-alignment for dual-polarized outdoor MIMO systems," in *IEEE GLOBECOM Workshops 2013*, Dec. 2013, pp. 356–361.

[6] A. Alkhateeb, O. E. Ayach, G. Leus, and R. W. Heath, "Channel estimation and hybrid precoding for millimeter wave cellular systems," *IEEE Journal of Selected Topics in Signal Processing*, vol. 8, no. 5, pp. 831–846, Oct. 2014.

[7] O. E. Ayach, S. Rajagopal, S. Abu-Surra, Z. Pi, and R. W. Heath, "Spatially sparse precoding in millimeter wave MIMO systems," *IEEE Transactions on Wireless Communications*, vol. 13, no. 3, pp. 1499–1513, March 2014.

[8] A. M. Sayeed, "Deconstructing multiantenna fading channels," *IEEE Transactions on Signal Processing*, vol. 50, no. 10, pp. 2563–2579, Oct. 2002.

[9] G. H. Song, J. Brady, and A. Sayeed, "Beamspace MIMO transceivers for low-complexity and near-optimal communication at mm-wave frequencies," in *2013 IEEE International Conference on Acoustics, Speech and Signal Processing (ICASSP)*, May 2013, pp. 4394–4398.

[10] T. Kim and D. Love, "Virtual AoA and AoD estimation for sparse millimeter wave MIMO channels," in *IEEE International Workshop on Signal Processing Advanced in Wireless Communications (SPAWC)*, Stockholm, Sweden, June 2015.

[11] T. Kim, D. Love, and B. Clerckx, "MIMO systems with limited rate differential feedback in slowly varying channels," *IEEE Transactions on Communications*, vol. 59, no. 4, pp. 1175–1189, April 2011.

[12] B. Banister and J. Zeidler, "Feedback assisted transmission subspace tracking for MIMO systems," *IEEE Jour. Select. Areas in Commun.*, vol. 21, no. 3, pp. 452–463, April 2003.

[13] J. Yang and D. Williams, "Transmission subspace tracking for MIMO systems with low-rate feedback," *IEEE Trans. Commun.*, vol. 55, no. 8, pp. 1629–1639, Aug. 2007.

[14] E. J. Candes, J. Romberg, and T. Tao, "Stable signal recovery from incomplete and inaccurate measurements," *Comm. Pure Appl. Math.*, vol. 59, pp. 1207–1223, Feb. 2006.

[15] M. Rossi, A. Haimovich, and Y. Eldar, "Spatial compressive sensing for MIMO radar," *IEEE Transactions on Signal Processing*, vol. 62, no. 2, pp. 419–430, Jan. 2014.

[16] D. Chu, "Polyphase codes with good periodic correlation properties," *IEEE Transactions on Information Theory*, vol. 18, no. 4, pp. 531–532, 1972.

[17] S. Beyme and C. Leung, "Efficient computation of DFT of Zadoff-Chu sequences," *Electronics Letters*, vol. 45, no. 9, pp. 461 –463, 23 2009.

[18] D. L. Donoho, A. Maleki, and A. Montanari, "Message passing algorithms for compressed sensing: I. motivation and construction," in *IEEE Information Theory Workshop (ITW)*, Jan. 2010, pp. 1–5.

[19] A. Maleki, L. Anitori, Z. Yang, and R. Baraniuk, "Asymptotic analysis of complex LASSO via complex approximate message passing (camp)," *IEEE Transactions on Information Theory*, vol. 59, no. 7, pp. 4290–4308, July 2013.